Original Article
Food Science and Technology

ISSN 0101-2061 (Print)
ISSN 1678-457X (Online)

DOI: https://doi.org/10.1590/fst.76422

Effect of cross-linking with sodium trimetaphosphate on structural and physicochemical properties of tigernut starch

Xiaofan LV[1], Yuzhen CHEN[1]*, Wei ZHOU[1]

Abstract

With sodium trimetaphosphate as cross-linking agent, the cross-linked tigernut starch (CLTS) was prepared in this study. The effects of cross-linking on the structure and physicochemical properties of tigernut starch were also investigated. FT-IR analysis confirmed the formation of CLTS. X-Ray diffraction (XRD) results suggested that cross-linking not only retained the crystallization type of starch (C-type), but also enhanced the crystallinity. Compared with the native tigernut starch (NTS), CLTS had lower solubility and swelling power, the better syneresis and freeze-thaw stability. It was more prone to settlement. The pasting temperature and peak viscosity of CLTS were superior to those of NTS. It was easier to regenerate at low temperature, and its thermal stability was also significantly improved. Our results provide a reference for the in-depth development of tigernut starch.

Keywords: tigernut; cross-linked starch; sodium trimetaphosphate; physicochemical properties.

Practical Application: The cross-linked tigernut starch (CLTS) with sodium trimetaphosphate was prepared. Its physicochemical properties of tigernut starch were also investigated. The results show that CLST is a kind of modified starch with potential application in the field of food.

1 Introduction

Starch is an important raw material for food processing. However, at present, only a few common starches were used in the production of commercial starch, such as potato starch, corn starch and so on, which greatly limits the development of starch and starch products. As a kind of multi-purpose crop with high comprehensive utilization value, tigernut has more comprehensive nutrients than wheat and corn, and its starch content is as high as 26%- 30% (Liu et al., 2019). Previous studies have found that tigernut starch has good gel properties, and it belongs to slow digestion starch, which can be used in functional foods to reduce postprandial blood glucose (Lv et al., 2022; Wang et al., 2022). However, like other natural starches, tigernut starch also has some inherent defects and needs to be modified.

The cross-linking reaction can enhance the binding between starch particles and make the starch molecules more stable. It can significantly improve the gelatinization temperature and thermal stability of starch. Cross-linked starch also has excellent freeze-thaw stability and anti-aging property, The addition of cross-linked starch can maintain moisture in food and prolong shelf life (Xie et al., 2019; Brasil et al., 2021). Sodium trimetaphosphate is a commonly used food additive with recognized safety and is often used as a cross-linking agent (Li et al., 2009; Xie et al., 2022). In this study, cross-linked tigernut starch (CLTS) was prepared with sodium trimetaphosphate as cross-linking agent, and the effects of cross-linking on the structure and physicochemical properties of tigernut starch were also investigated in order to promote the application of tigernut starch.

2 Materials and methods

2.1 Materials and chemicals

Tigernut starch (variety, Yuyousha 1) was from Henan Academy of Agricultural Sciences (Zhengzhou, China); Sodium trimetaphosphate was purchased from Shanghai Yuanye Biotechnology Co., Ltd. (Shanghai, China). Other chemicals were of analytical grade.

2.2 Preparation of CLTS

NTS was suspended in distilled water at 40% (w/w), and adjusted to pH of 10.2, mixed with sodium trimetaphosphate (1.5% of starch dry basis). The mixture was kept at 45 °C and oscillated for 2 h. Finally, the pH of the mixture was adjusted to 6.5 with 0.5 mol/L HCl. It was washed 4 times by distilled water, filtered, dried at 45 °C for 12 h, crushed through a 100-mesh sieve, and collected as CLTS.

2.3 FT-IR measurement

The FT-IR spectra of NTS and CLTS in the range of 500-4000 cm^{-1} were obtained by the KBr disc method using a Bruker INVENIOR infrared spectrophotometer (Karlsruhe, Germany) with 64 scans and the resolution of 4 cm^{-1} (Li et al., 2019).

2.4 XRD measurement

The XRD patterns of NTS and CLTS in the 2θ range of 5°~45° were measured by a Bruker D8 Advance X-ray diffractometer

Received 12 June, 2022
Accepted 02 Aug., 2022
[1] *Henan Institute of Science and Technology, Xinxiang, China*
*Corresponding author: cyz_dlut@126.com

(Karlsruhe, Germany) at 40 kV and 40 mA with Cu Ka radiation. The degree of relative crystallinity was calculated by using MDI-Jade 6.0 software (Material Date, Inc. Livermore, California, USA) (Miao et al., 2009).

2.5 Determination of settling volume

The settling volume of the sample was determined by the method of Shukri & Shi (2015). 1.2 g starch and 118.2 mL distilled water were evenly mixed, heated at 95 °C, stirred for 30 min, and then cooled to room temperature. The 100 mL of the obtained starch paste was placed in a measuring cylinder and the settling volume was read after 24 h.

2.6 Determination of paste clarity

The starch was suspended in distilled water at 1% (w/w), heated in a boiling water bath for 15 min with constant stirring, and cooled down to room temperature. Its transmittance (%) was recorded at 620 nm to indicate the paste clarity (Correia et al., 2012).

2.7 Determination of syneresis

The starch was suspended in distilled water at 2% (w/w), heated in a boiling water bath for 20 min with constant stirring. Then, a certain amount of starch paste (W_{paste}) was stored it in refrigerator at 4 °C for 24 h, and then centrifuged at 4000 rpm for 15 min. The weight of separated water was recorded (W_{sw}). The syneresis (SYV) could be calculated by the following equation (Jing et al., 2012) (Equation 1).

$$SYV = \frac{W_{sw}}{W_{paste}} \times 100\% \quad (1)$$

2.8 Measurement of freeze-thaw stability

The starch suspension (6.0%, w/w) was heated in a boiling water bath and stirred for 15 min. After cooled to room temperature, a certain amount of starch paste (W_{paste}) was placed in the centrifugal tube, kept in the refrigerator at -18 °C for 24 h, thawed at room temperature for 2 h, and then centrifuged at 6000 rpm for 15 min. The supernatant (W_{water}) was collected and weighed. Finally, the freeze-thaw stability (FTS) was calculated by the following equation (Luo et al., 2006) (Equation 2).

$$FTS = \frac{W_{water}}{W_{paste}} \times 100\% \quad (2)$$

2.9 Solubility and swelling power

A certain amount of starch ($W_{initial}$) was dissolved in water to prepare 2% starch suspension (2%, w/w), which was heated to 30 min at 50, 60, 70, 80, 90 °C, respectively. After cooled to room temperature, it was centrifuged at 6000 rpm for 15 min. The supernatant was poured into a constant weight glass weighing dish and dried at 105 °C to constant weight (W_{solube}). The residue in the centrifuge tube was also weighted as $W_{swollen}$. The solubility (SOL) and swelling degree (SP) of sample could be calculated according to the following formula (Singh et al., 2009) (Equations 3-4).

$$SOL = \frac{W_{solube}}{W_{initial}} \times 100\% \quad (3)$$

$$SP = \frac{W_{swollen}}{W_{initial}(1 - SOL)} \times 100\% \quad (4)$$

2.10 Evaluation of pasting properties

The pasting properties of sample was measured by a Perten RVA 4500 (Stockholm, Sweden). 3.0 g starch was fully mixed with 25 mL distilled water, put into RVA, and determined by RVA Super3 Standards program: the sample was kept 1 min at 50 °C, then heated to 95 °C after 3.5 min, kept at 95 °C for 3 min, then decreased to 50 °C after 3.5 min, and then kept at 50 °C for 2 min, the whole process lasted 13 min (Wang & Copeland, 2012).

2.11 Statistical analysis

The experimental results were expressed as the average ± standard deviation (n = 3). The statistical comparison was based on the Tukey method with a confidence level of 95%.

3 Results and discussion

3.1 FT-IR analysis

Figure 1 exhibits FT-IR spectra of NTS and CLTS. The characteristic peak at 3402 cm^{-1} of NTS was from the stretching vibration of -OH, the peak at 2928 cm^{-1} represented the stretching vibration of -CH, the peaks at 1157 cm^{-1}, 1082 cm^{-1}, 1017 cm^{-1} were due to expansion vibration of C=O bond (Li et al., 2022), these characteristic peaks still could be found in the FT-IR spectrum of CLTS. Moreover, the stretching vibration of CLTS at 3402 cm^{-1} increased, which was attributed to the cross-linking between the phosphate group of sodium trimetaphosphate and the hydroxyl group of starch. The stretching vibration of CLTS at 1050-970 cm^{-1} was also stronger than that of NTS, which was caused by the stretching vibration of P-O-C bond.

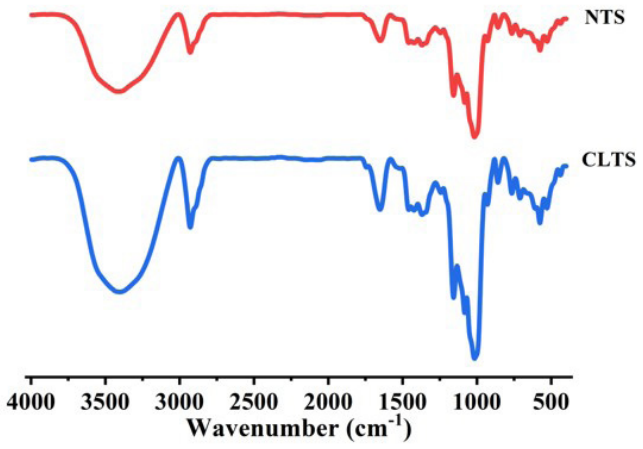

Figure 1. FT-IR spectra of NTS and CLTS.

It could be concluded that NTS was connected with phosphate bond after cross-linking reaction, which was consistent with the previous report (Gao et al., 2014). The absorbance ratio of sample at 1047 and 1022 nm ($R_{1047/1022}$) in the FT-IR spectrum was usually used to characterize the short-range molecular order of starch, the larger the ratio, the higher the order of starch (Van Soest et al., 1995). The $R_{1047/1022}$ of CLTS (1.026) was superior to that of NTS (1.001). After cross-linking, starch molecules formed a multi-dimensional spatial structure, which made the knots between starch molecules closer and enhanced the order of its short-range.

3.2 XRD analysis

Figure 2 demonstrates the XRD patterns of NTS and CLTS. NTS had the sharp diffraction peaks of NTS at 15°, 17° and 23°, which did not changed significantly in the XRD spectrum of CLTS, indicating that the cross-linking reaction did not change the crystal type of NTS, and it was still C-type starch. Our results was consistent with the previous report (Lv et al., 2022). However, the crystallinity of CLTS (12.4%) was higher than that of NTS (11.3%). This change may be due to the fact that the cross-linking reaction mainly occurred in the crystalline region of starch (Koo et al., 2010), and the formation of diester bonds strengthened the structure of starch (Liu et al., 2022), which was also confirmed by FT-IR results.

3.3 Settling volume

It is difficult to measure the cross-linking degree of cross-linked starch, but there is a linear negative correlation between cross-linking degree and settling volume of starch (Geng et al., 2022). Therefore, the settling volume can be used to reflect the cross-linking degree of cross-linked starch. As shown in Table 1, the settling volume of CLTS (2.51 ± 0.11 mL/g) was lower than that of NTS (2.93 ± 0.10 mL/g). The decrease of the settling volume was caused by the cross-linking reaction, which inhibited the swelling of starch (Wang et al., 2018).

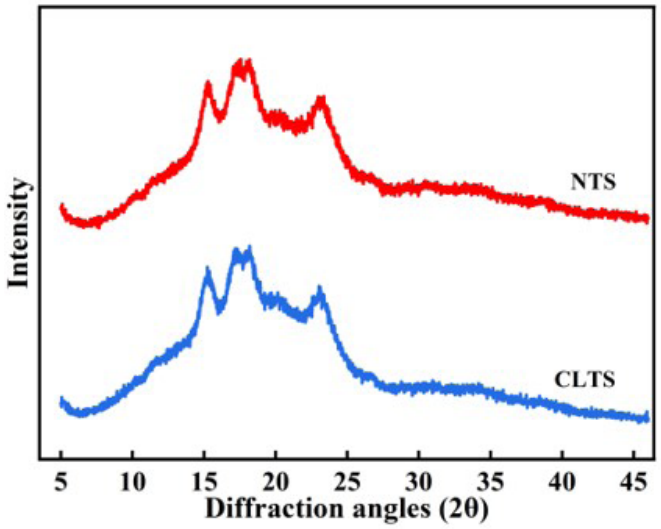

Figure 2. XRD patterns of NTS and CLTS.

Table 1. Physicochemical properties of NTS and CLTS.

	Settling volume (mL/g)	Clarity (%)	Syneresis (%)	Freeze-thaw stability (%)
NTS	2.93 ± 0.10	3.04 ± 0.13	32.18 ± 0.46	47.42 ± 3.66
CLTS	2.51 ± 0.11	2.31 ± 0.06	25.52 ± 1.12	29.75 ± 3.35

3.4 Paste clarity

Starch paste clarity was an important index to evaluate starch products. The source of starch, the color of starch itself, the form of starch in starch paste and the groups introduced after starch denaturation all affect the paste clarity of starch. In Table 1, the light transmittance of CLTS was lower than that of NTS, which may be due to the introduction of the cross-linked bond of starch. These bonds enhanced the intermolecular interaction of starch (Carmona-Garcia et al., 2009), and improved integrity of the gelatinized starch. As a result, it made the starch difficult to expand, the scattering of starch was enhanced, and the paste clarity of starch was reduced (Ogunmolasuyi et al., 2017).

3.5 Syneresis

After the gelatinized starch was placed at room temperature, the starch molecules were rearranged and insoluble precipitates were formed by hydrogen bonding, which can be reflected by syneresis value of starch. The syneresis value of starch was affected by amylose content, molecular structure, water content and starch aging time. As shown in Table 1, the syneresis value of CLTS was lower than that of NTS. It may be attributed to the formation of starch phosphate, delaying the aging of starch (Wiesenborn et al., 1994).

3.6 Freeze-thaw stability

During the process of freezing and thawing, the water precipitation rate was negatively proportional to the freeze-thaw stability. Compared with NTS, the freeze-thaw stability of CLTS was significantly improved. The phosphate group introduced by the cross-linking reaction prompted the formation of three-dimensional network structure of starch, which led to the steric hindrance of starch molecules and made the dispersion system of starch paste more stable (Liu & Zhang, 2006). As a result, the freeze-thaw stability of starch paste was improved.

3.7 Solubility and swelling power

The solubility and swelling power of starch were related to its starch particle size, molecular structure and molecular mass, reflecting the interaction between starch and water. As shown in Figure 3, the solubility and swelling power of starch gradually ascended with the increase of temperature, but the solubility and swelling power of CLTS was lower than that of NTS at the same temperature. During the process of gelatinization of starch, the intermolecular hydrogen bonding decreased, starch particles absorbed water and expanded, and a small part of starch dissolved in water. After cross-linking, the solubility and swelling power of starch particles were inhibited (Koo et al., 2010). Xie et al.

Table 2. Pasting properties of NTS and CLTS.

	Pasting temperature (°C)	Peak	Though	Final	Breakdown	Setback
NTS	78.07 ± 0.49	2929 ± 6.08	2098 ± 14.80	3249 ± 29.24	831 ± 12.77	1151 ± 16.01
CLTS	86.68 ± 1.03	2951 ± 14.36	2253 ± 42.58	4895 ± 82.50	698 ± 32.19	2642 ± 123.62

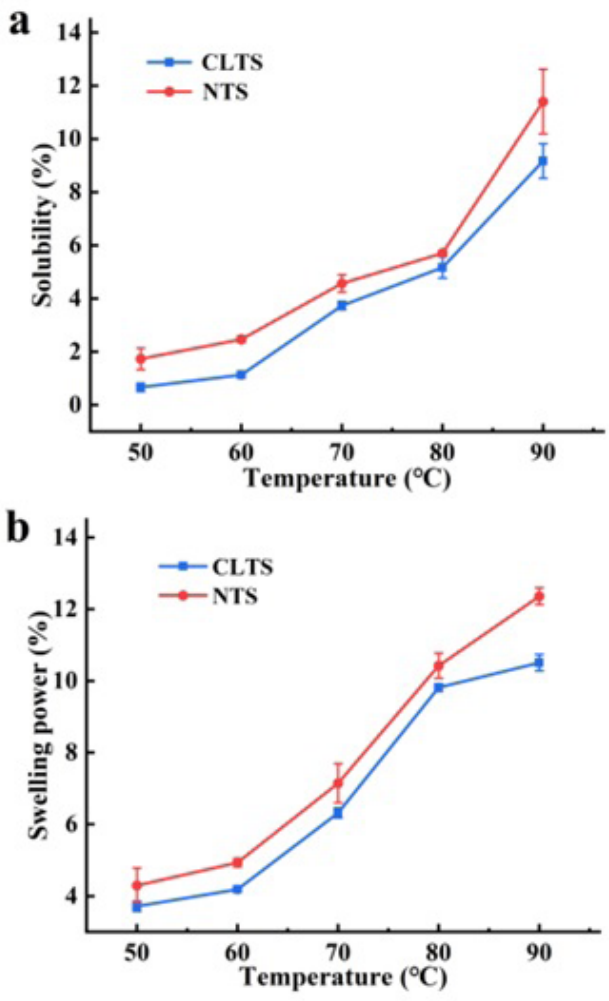

Figure 3. Solubility (a) and swelling power (b) of NTS and CLTS.

(2019) also found that the cross-linking reaction with sodium trimetaphosphate could enhance the interaction between starch chains and restrain the swelling power.

3.8 Pasting properties

The paste temperature, peak viscosity and setback of starch all determined the usable range of starch. During the gelatinization process, the internal components of starch exudated and formed a three-dimensional network structure with the expansion of particle volume, and the pasting property of starch was affected by its amylose content, particle size, molecular forces and other factors (Cai et al., 2014; Wang et al., 2018). In Table 2, the peak viscosity, though viscosity, final viscosity, set back and pasting temperature of CLTS were all higher than those of NTS, indicating that its viscosity increased after cross-linking and it was easier to retrogradate at low temperature. After cross-linking, there were not only hydrogen bonds but also covalent bonds among starch molecules, which strengthened the interaction between starch and water during gelatinization, and the energy required for starch phase change was greater (Jyothi et al., 2006). The breakdown of CLTS was lower than that of NTS, which also suggested that the thermal stability of CLTS was significantly improved. Kou & Gao (2018) reported that the cross-linking reaction of starch could improve the peak viscosity of starch and the overall stability of starch paste, which coincided with our results.

4 Conclusion

In this study, sodium trimetaphosphate was used as cross-linking agent to prepare CLTS, XRD and FTIR analysis showed that the cross-linking reaction mainly occurred in the crystal region of starch, and did not change the crystal type of starch. After cross-linking, syneresis value, freeze-thaw stability, pasting temperature and peak viscosity of the starch were improved, and CLTS was easier to regenerate and settle. Because of the introduction of phosphate group, CLTS was not easy to gelatinize, and the stability and integrity of starch particle structure were maintained, and the solubility and swelling power of starch were inhibited, and the thermal stability of starch paste was also improved. This study provided a reference for the further development of NTS.

Funding

This work was supported by Natural Science Foundation of Henan (No.202300410158), the Training Plan of Young Key Teachers in Henan (No.2020GGJS167), and the Scientific and Technological Project in Henan Province of China (No. 222102110104).

References

Brasil, V. C. B., Guimarães, B. P., Evaristo, R. B. W., Carmo, T. S., & Ghesti, G. F. (2021). Buckwheat (*Fagopyrum esculentum Moench*) characterization as adjunct in beer brewing. *Food Science and Technology*, 41(Suppl. 1), 265-272. http://dx.doi.org/10.1590/fst.15920.

Cai, J., Cai, C., Man, J., Zhou, W., & Wei, C. (2014). Structural and functional properties of C-type starches. *Carbohydrate Polymers*, 101, 289-300. http://dx.doi.org/10.1016/j.carbpol.2013.09.058. PMid:24299776.

Carmona-Garcia, R., Sanchez-Rivera, M. M., Méndez-Montealvo, G., Garza-Montoya, B., & Bello-Pérez, L. A. (2009). Effect of the cross-linked reagent type on some morphological, physicochemical and functional characteristics of banana starch (Musa paradisiaca). *Carbohydrate Polymers*, 76(1), 117-122. http://dx.doi.org/10.1016/j.carbpol.2008.09.029.

Correia, P. R., Nunes, M. C., & Beirão-da-Costa, M. L. (2012). The effect of starch isolation method on physical and functional properties of Portuguese nuts starches. I. Chestnuts (Castanea sativa Mill. var. Martainha and Longal) fruits. *Food Hydrocolloids*, 27(1), 256-263. http://dx.doi.org/10.1016/j.foodhyd.2011.05.010.

Gao, F., Li, D., Bi, C. H., Mao, Z. H., & Adhikari, B. (2014). Preparation and characterization of starch crosslinked with sodium trimetaphosphate and hydrolyzed by enzymes. *Carbohydrate Polymers*, 103, 310-318. http://dx.doi.org/10.1016/j.carbpol.2013.12.028. PMid:24528734.

Geng, S., Li, Y., Lv, J., Ma, H., Liang, G., & Liu, B. (2022). Fabrication of food-grade Pickering high internal phase emulsions (HIPEs) stabilized by a dihydromyricetin and lysozyme mixture. *Food Chemistry*, 373(Pt B), 131576. http://dx.doi.org/10.1016/j.foodchem.2021.131576. PMid:34799133.

Jing, S., Yan, X., Ouyang, W., Xiang, H., & Ren, Z. (2012). Study on properties of Cyperus esculentus starch grown in Xinjiang, China. *Stärke*, 64(8), 581-589. http://dx.doi.org/10.1002/star.201100129.

Jyothi, A. N., Moorthy, S. N., & Rajasekharan, K. N. (2006). Effect of cross-linking with epichlorohydrin on the properties of cassava (Manihot esculenta Crantz) starch. *Stärke*, 58(6), 292-299. http://dx.doi.org/10.1002/star.200500468.

Koo, S. H., Lee, K. Y., & Lee, H. G. (2010). Effect of cross-linking on the physicochemical and physiological properties of corn starch. *Food Hydrocolloids*, 24(6-7), 619-625. http://dx.doi.org/10.1016/j.foodhyd.2010.02.009.

Kou, T., & Gao, Q. (2018). New insight in crosslinking degree determination for crosslinked starch. *Carbohydrate Research*, 458-459, 13-18. http://dx.doi.org/10.1016/j.carres.2018.01.009. PMid:29428482.

Li, B. Z., Wang, L. J., Li, D., Chiu, Y. L., Zhang, Z. J., Shi, J., Chen, D. X., & Mao, Z. H. (2009). Physical properties and loading capacity of starch-based microparticles crosslinked with trisodium trimetaphosphate. *Journal of Food Engineering*, 92(3), 255-260. http://dx.doi.org/10.1016/j.jfoodeng.2008.10.008.

Li, J., Geng, S., Zhen, S., Lv, X., & Liu, B. (2022). Fabrication and characterization of oil-in-water emulsions stabilized by whey protein isolate/phloridzin/sodium alginate ternary complex. *Food Hydrocolloids*, 129, 107625. http://dx.doi.org/10.1016/j.foodhyd.2022.107625.

Li, X. M., Zhu, J., Pan, Y., Meng, R., Zhang, B., & Chen, H. Q. (2019). Fabrication and characterization of pickering emulsions stabilized by octenyl succinic anhydride-modified gliadin nanoparticle. *Food Hydrocolloids*, 90, 19-27. http://dx.doi.org/10.1016/j.foodhyd.2018.12.012.

Liu, D., & Zhang, L. (2006). Structure and properties of soy protein plastics plasticized with acetamide. *Macromolecular Materials and Engineering*, 291(7), 820-828. http://dx.doi.org/10.1002/mame.200600098.

Liu, X. X., Liu, H. M., Li, J., Yan, Y. Y., Wang, X. D., Ma, Y. X., & Qin, G. Y. (2019). Effects of various oil extraction methods on the structural and functional properties of starches isolated from tigernut (*Cyperus esculentus*) tuber meals. *Food Hydrocolloids*, 95, 262-272. http://dx.doi.org/10.1016/j.foodhyd.2019.04.044.

Liu, X., Geng, S., He, C., Sun, J., Ma, H., & Liu, B. (2022). Preparation and characterization of a dihydromyricetin–sugar beet pectin covalent polymer. *Food Chemistry*, 376, 131952. http://dx.doi.org/10.1016/j.foodchem.2021.131952. PMid:34973639.

Luo, Z., He, X., Fu, X., Luo, F., & Gao, Q. (2006). Effect of microwave radiation on the physicochemical properties of normal maize, waxy maize and amylomaize V starches. *Stärke*, 58(9), 468-474. http://dx.doi.org/10.1002/star.200600498.

Lv, X., Zhang, S., Zhen, S., Shi, Y., & Liu, B. (2022). Physicochemical properties of tigernut (Cyperus esculentus) tuber starch and its application in steamed bread. *Journal of Food Processing and Preservation*, e16792. Ahead of print. http://dx.doi.org/10.1111/jfpp.16792.

Miao, M., Zhang, T., & Jiang, B. (2009). Characterisations of kabuli and desi chickpea starches cultivated in China. *Food Chemistry*, 113(4), 1025-1032. http://dx.doi.org/10.1016/j.foodchem.2008.08.056.

Ogunmolasuyi, A. M., Egwim, E. C., Adewoyin, M. A., & Nkop, J. E. (2017). Effect of phosphoric acid treatment on physicochemical, functional, and structural properties of starch extracted from yam (*Dioscorea rotundata*). *International Journal of Food Properties*, 20(5), 1062-1073. http://dx.doi.org/10.1080/10942912.2016.1199035.

Shukri, R., & Shi, Y. C. (2015). Physiochemical properties of highly cross-linked maize starches and their enzymatic digestibilities by three analytical methods. *Journal of Cereal Science*, 63, 72-80. http://dx.doi.org/10.1016/j.jcs.2015.03.001.

Singh, N., Singh, S., Isono, N., Noda, T., & Singh, A. M. (2009). Diversity in amylopectin structure, thermal and pasting properties of starches from wheat varieties/lines. *International Journal of Biological Macromolecules*, 45(3), 298-304. http://dx.doi.org/10.1016/j.ijbiomac.2009.06.005. PMid:19549541.

Van Soest, J. J. G., Tournois, H., Wit, D., & Vliegenthart, J. F. G. (1995). Short-range structure in (partially) crystalline potato starch determined with attenuated total reflectance Fourier-transform IR spectroscopy. *Carbohydrate Research*, 279, 201-214. http://dx.doi.org/10.1016/0008-6215(95)00270-7.

Wang, S., & Copeland, L. (2012). Effect of alkali treatment on structure and function of pea starch granules. *Food Chemistry*, 135(3), 1635-1642. http://dx.doi.org/10.1016/j.foodchem.2012.06.003. PMid:22953904.

Wang, S., Guo, L., Miao, Z., Ma, H., & Melnychuk, S. (2022). Effects of maternal vitamin D3 status on quality characteristics of pork batters in offspring pigs during cold storage. *Food Science and Technology*, 42, e102021. http://dx.doi.org/10.1590/fst.102021.

Wang, W., Guan, L., Seib, P. A., & Shi, Y. C. (2018). Settling volume and morphology changes in cross-linked and unmodified starches from wheat, waxy wheat, and waxy maize in relation to their pasting properties. *Carbohydrate Polymers*, 196, 18-26. http://dx.doi.org/10.1016/j.carbpol.2018.05.009. PMid:29891286.

Wiesenborn, D. P., Orr, P. H., Casper, H. H., & Tacke, B. K. (1994). Potato starch paste behavior as related to some physical/chemical properties. *Journal of Food Science*, 59(3), 644-648. http://dx.doi.org/10.1111/j.1365-2621.1994.tb05583.x.

Xie, D., Lei, Y., & Sun, Y. (2022). Effects of heating method and refrigerating time on nutritional quality and digestive characteristics of refrigerated Chinese steamed bread. *Food Science and Technology*, 42, e10122. http://dx.doi.org/10.1590/fst.10122.

Xie, Y., Zhang, B., Li, M. N., & Chen, H. Q. (2019). Effects of cross-linking with sodium trimetaphosphate on structural and adsorptive properties of porous wheat starches. *Food Chemistry*, 289, 187-194. http://dx.doi.org/10.1016/j.foodchem.2019.03.023. PMid:30955602.